AAPS PharmSciTech, Vol. 16, No. 2, April 2015 (© 2014)
DOI: 10.1208/s12249-014-0223-7

Research Article

Development and Characterization of Sorbitan Monostearate and Sesame Oil-Based Organogels for Topical Delivery of Antimicrobials

Vinay K. Singh,[1] Krishna Pramanik,[1] Sirsendu S. Ray,[1] and Kunal Pal[1,2]

Received 12 June 2014; accepted 12 September 2014; published online 4 October 2014

Abstract. The current study explains the development of sorbitan monostearate and sesame oil-based organogels for topical drug delivery. The organogels were prepared by dissolving sorbitan monostearate in sesame oil (70°C). Metronidazole was used as a model antimicrobial. The formulations were characterized using phase contrast microscopy, infrared spectroscopy, viscosity, mechanical test, and differential scanning calorimetry. Phase contrast microscopy showed the presence of needle-shaped crystals in the organogel matrix. The length of the crystals increased with the increase in the sorbitan monostearate concentration. XRD studies confirmed the amorphous nature of the organogels. Viscosity study demonstrated shear thinning behavior of the organogels. The viscosity and the mechanical properties of the organogels increased linearly with the increase in the sorbitan monostearate concentration. Stress relaxation study confirmed the viscoelastic nature of the organogels. The organogels were biocompatible. Metronidazole-loaded organogels were examined for their controlled release applications. The release of the drug followed zero-order release kinetics. The drug-loaded organogels showed almost similar antimicrobial activity against *Escherichia coli* when compared to the commercially available Metrogyl® gel. In gist, it can be proposed that the developed organogels had sufficient properties to be used for controlled delivery of drugs.

KEY WORDS: organogel; phase contrast microscopy; sesame oil; sorbitan monostearate.

INTRODUCTION

Gels are semisolid formulations prepared by dispersing a micromolecular liquid in a three-dimensional (3-D) network of a solid component, which forms a supramolecular 3-D architecture. The molecules of the solid component generally undergo strong intermolecular bonding (physical force) or forms chemical bonds. This results in the cross-linking of the solid molecules to form a 3-D architecture (1).

Immobilization of the liquid component inside the networked arrangement of the solid constituent can be credited to the interfacial activity between the solid and liquid constituents (2). The liquid phase may either be polar or apolar. If the liquid phase is polar in nature, then the gels are called as hydrogels, otherwise, organogels (3). The solid components are named as gelator (4). Organogels offer numerous advantages over conventional gel compositions. Due to the absence of polar phase, they are safe from bacterial attacks and hence do not require addition of preservatives. Organogels are reported to have numerous applications in pharmaceutical, nutraceutical, food, and cosmetic industries (5).

Organogels have been investigated successfully as dermal pharmaceutical formulations (6). The formulations designed for topical applications should be able to interact with the skin, which acts as an anatomical and biological barrier for drug penetration to the systemic circulation. Many organic substances, like lipids, work as a penetration enhancer. The cosmetics industry employs organogels in personal care products like sunscreens, lipsticks, and moisturizers (7).

The food industry utilizes organogel-based products for structuring edible oils at low concentrations of the gelator molecules. The commonly used organogelators include monoacylglycerols, diacylglycerols, triacylglycerols (8), fatty acids (9), fatty alcohols (9), waxes, wax esters (10), and sorbitan monostearate (8).

Sorbitan monostearate (SMS) is a non-ionic surfactant which is hydrophobic in nature and forms organogel of organic solvents (e.g., hexadecane, isopropyl myristate, and a range of vegetable oils like sesame oil, groundnut oil, olive oil, soybean oil, sunflower oil) (11, 12). Sorbitan monostearate-based organogels have also been developed for pharmaceutical applications (13, 14).

Sesame oil is obtained from the ripe seeds of *Sesamum indicum* L. Sesame seeds contain the highest oil (44–58%) among the primary edible oils along with proteins (18–25%) and carbohydrates (13.5%) (15). Sesame oil has been used

Electronic supplementary material The online version of this article (doi:10.1208/s12249-014-0223-7) contains supplementary material, which is available to authorized users.

[1] Department of Biotechnology and Medical Engineering, National Institute of Technology, Rourkela, Odisha 769008, India.
[2] To whom correspondence should be addressed. (e-mail: pal.kunal@yahoo.com; kpal.nitrkl@gmail.com)

extensively for pharmaceutical and cosmetic applications due to its antiseptic, disinfectant, antiinflammatory, antitubercular, antiviral, antibacterial, and antioxidant properties (16). The major components of sesame oil (sesamin, sesamolin, and sesamol) provide stability against oxidative deterioration of the formulations (17, 18). Sesame oil has the highest antioxidant content among the primary edible oils (19). It also contains abundant fatty acids such as oleic acid (43%), linoleic acid (35%), palmitic acid (11%), and stearic acid (7%) (15). It possesses a distinct flavor which makes it a suitable candidate to be used in the food industry (16). These characteristics have drawn the interest of many scientists to use sesame oil in various pharmaceuticals, cosmetics, and food products (20). Sesamin, a major lignan present in sesame oil, is reported to show cholesterol-lowering and antihypertensive activities (21). Chen *et al.* reported a significant decrease in the serum total cholesterol levels and low-density lipoprotein cholesterol in the diet supplemented with sesame oil. It also enhanced the antioxidant capacity in hypercholesterolemic patients (22). Tsuruoka *et al.* suggested that sesamin regulates lipid metabolism, xenobiotics, and alcohol at the messenger RNA (mRNA) level (21). Periasamy *et al.* reported protection against sinusoidal obstruction syndrome by downregulating matrix metalloproteinase-9 expression, upregulating TIMP-1 expression, and inhibiting oxidative stress by a single prophylactic dose of sesame oil (23). Saleem *et al.* demonstrated antioxidant and tumor necrosis factor alpha-inhibiting activity of sesame oil against acute doxorubicin-induced cardiotoxicity by enhancing cardiac endogenous antioxidants and decreasing myocardial TNF-α expression (24).

Keeping these facts into consideration, the current study reports the development of the organogels using sorbitan monostearate as the organogelator and sesame oil as the organic phase. To the best of our knowledge, sorbitan monostearate and sesame oil-based organogels have not been reported so far. The presence of sesame oil may impart its beneficial effects when the organogel is applied topically. The organogels were developed by varying the concentration of sorbitan monostearate. The stable organogels were characterized using various techniques such as microscopy, Fourier transform infrared (FTIR) spectroscopy, viscosity, mechanical properties, and differential scanning calorimetry. Metronidazole, a model antimicrobial drug, was incorporated into the organogels. The release of the drug from the organogel was checked by *in vitro* release studies. The qualitative release study was done to understand the antimicrobial efficacy of the drug-loaded formulations.

MATERIALS AND METHOD

Materials

Sorbitan monostearate was obtained from Loba Chemie Pvt. Ltd., Mumbai, India. Food-grade sesame oil (Tilsona®) was obtained from Recon Oil Industries Pvt. Ltd., Mumbai, India. Metronidazole was kindly provided by Aarti Drugs, Mumbai, India. All the chemicals were used as received. Nutrient agar was received from HiMedia Laboratories Pvt. Ltd., Mumbai, India. The microbial culture of *Escherichia coli* (NCIM 2563) was obtained from the National Collection of Industrial Microorganism (NCIM), Pune, India. Milli-Q water was used throughout the study.

Methods

Preparation of Organogel

The required quantity of sorbitan monostearate was dissolved in sesame oil (70°C, 500 RPM). The stirring was continued for 15 min under similar experimental condition to obtain a homogenous transparent mixture. The optimization of the composition of the organogel was done by varying the concentration of sorbitan monostearate from 5% *w*/*w* to 22% *w*/*w*. The minimum gelator (SMS) concentration required for inducing gelation is called the critical gelator concentration (CGC). The compositions tested for the gel formation are shown in Table I. The hot mixture when cooled to room temperature forms organogel at the sorbitan monostearate concentration ≥CGC. The formulations which did not show flow on inversion were selected as the representative samples for further characterization. The organogels were examined for their organoleptic properties like odor, color, texture, pH, oil leakage, phase separation, and tendency to flow (25).

Metronidazole was added to the organogels as a model antimicrobial drug at a concentration of 1% *w*/*w*. The drug-loaded organogels were prepared in a similar way. The drug was uniformly dispersed in sesame oil before adding sorbitan monostearate.

Stability Studies

The stability of the organogels was evaluated by accelerated stability study (freeze-thaw method) and intermediate stability study (incubated at 30±2°C/65±5% RH for 6 months as per ICH guidelines). The organogels were evaluated by physical observation (color, odor, texture, consistency), viscosity, oil leakage, phase separation, or any other sign of destabilization after each cycle of freeze-thaw thermocycling and at predefined time intervals (0, 1, 2, 3, and 6 months) during intermediate stability study (26).

Gelation Kinetics Study

The kinetics of gelation was studied by visible spectroscopy. A spectrophotometric scan was performed in the visible range (400–700 nm) to find the absorbance maxima of sesame oil. The organogels were molten and their absorbance was measured on a timescale for 2.5 min at an interval of 5 s during

Table I. Optimization of Organogel Formulations

Formulations	SMS (%)	Sesame oil (%)
T1	5	95
T2	10	90
T3	12.5	87.5
T4	15	85
T5	18	82
T6	20	80
T7	22	78

the cooling process. The scanning was carried out at the absorbance maxima of sesame oil. A constant weight (2.5 g) of organogels was used for the entire experiment.

Microscopic Studies

The microstructure of the organogels was studied using phase contrast microscopy (Primo Vert, Zeiss) equipped with camera (Axio Cam ERc5s). Thin smears of the organogel were prepared on glass slides and observed under ×40 magnification (27).

Fourier Transform Infrared Spectroscopy

The infrared spectra of the prepared organogels were recorded in the range of 400–4000 cm^{-1} using Bruker ALPHA-E FTIR spectrophotometer (USA) being operated in the attenuated total reflectance (ATR) mode. The spectrum was generated by accumulating 32 scans with a resolution of 4 cm^{-1}. The background measurements were subtracted from the actual sample measurement (28, 29).

Mechanical Properties

The mechanical properties of the developed organogels were studied using a cone and plate viscometer (Bohlin Visco 88, Malvern, UK) (30) and static mechanical tester (Stable MicroSystems, TA-HDplus, UK) at room temperature as per the reported literature (31). The study using a static mechanical tester was performed according to the protocol shown in Table S1. Cyclic creep and recovery studies were performed to assess the rheological properties of the organogels. The study was done by applying a constant force of 50 g using a cylindrical probe (diameter, 30 mm) in auto force mode (3 g) for 5 min (creep) followed by 5 g force for the next 5 min (recovery). The creep and the recovery studies were repeated for 10 cycles.

Thermal Properties

The melting points of the organogels were determined by the drop-ball method using a melting point apparatus (model-931, EI, India) (32). The differential scanning calorimetry (DSC) study was performed using DSC 200F3 Maia, Netzsch, Germany. The organogels (~15 mg) were hermetically sealed in aluminum pans, with pierced lids. The melting and crystallization events were recorded in the temperature range of 25°C–150°C at a thermal scanning rate of 5.0°C min^{-1} (27).

Biocompatibility Study

Biocompatibility evaluation of the organogels was done using HaCaT cell lines. The leachants of the organogels were prepared by extraction in phosphate buffer saline (pH 7.2) for 24 h. Cells were seeded in a 96-well plate at a density of 1.0×10^4 cells per well in the presence of Dulbecco's modified eagle medium supplemented with 10% fetal bovine serum. It was then kept in a humidified chamber supplied with 5% CO_2 maintained at 37°C. Then, 20 µl of the organogel extracts was added to each well and kept for incubation for 24 h. The culture medium was replaced with fresh medium and 100 µl of 3-(4,5-dimethylthiazol-2-yl)-2,5-diphenyltetrazolium bromide (MTT) dye was added to each well. It was incubated for 3 h of at 37°C and then the media were discarded. To this, 200 µl of dimethyl sulfoxide (DMSO) was added, which dissolves the insoluble formazan crystals and formed a purple-colored solution (33). The complete medium was taken as control. The cell viability was assessed with respect to the control by measuring the absorbance of the colored solution of formazan crystals in DMSO at 570 nm using a microplate reader (Multiskan EX, Thermo Scientific, Shanghai, China) (34).

In vitro Drug Release Studies

In vitro release studies of metronidazole from the organogel were performed using a modified Franz diffusion cell. The apparatus consisted of donor and receptor chambers. Accurately weighed (~1.0 g) samples were placed in the donor chamber attached to a previously activated dialysis membrane. The receptor chamber was filled with 50 ml of the dissolution media (phosphate buffer saline, pH 6.8), kept under stirring at 100 RPM (37°C). The donor chamber was brought closer to the receptor chamber, such that the dialysis membrane attached to the donor chamber just touched the dissolution media. The complete media were replaced with fresh media at predetermined time intervals and a small quantity (5 ml) was stored under refrigeration (2°C–8°C) for spectroscopic measurement. The study was performed for 12 h. The stored samples were filtered through a 0.45-µm Millipore filter and assayed using a UV–vis spectrophotometer (UV 3200 double beam, Lab India) at 321 nm (35).

Antimicrobial Study

Metronidazole-loaded organogels were tested for their antimicrobial efficacy against *E. coli* according to the literature reported elsewhere (26). Two controls were taken, a positive (commercially available metronidazole gel, Metrogyl®) and a negative (blank organogel) control. The petri plates were incubated under aerobic conditions at 37°C for 24 h. The zone of inhibition was measured at the end of 12 h of incubation and compared with the positive and the negative controls (36).

RESULTS AND DISCUSSION

Preparation of the Organogels

The formulations containing lower concentrations of sorbitan monostearate (<15% *w/w*) resulted in the phase separation. The formulations did not form organogels when cooled to room temperature (25°C). At a gelator concentration ≥15% (*w/w*), organogels were formed when the hot mixture of sorbitan monostearate and sesame oil was slowly cooled down to room temperature. The solution of sorbitan monostearate and sesame oil was transparent when hot, which slowly turned turbid and finally converted into organogel (opaque). In general, water-devoid organogels require a high gelator concentration to induce gelation. Shah *et al.* found the minimum sorbitan monostearate concentration to be 20% *w/w* using olive oil as apolar phase (13). Behera *et al.* used 18% *w/w* of sorbitan monostearate for preparing sunflower oil-based

organogels (37). The organogels were slightly yellowish in color and were smooth in texture (Figure S1). The organogel formulations were selected for further analysis (Table II).

A concentration-dependent change was observed in the physical properties of the prepared organogels. The consistency and smoothness of the organogels increased with the increase in the concentration of the sorbitan monostearate. The organogels with lower proportions of sorbitan monostearate were easily spreadable. The organogels containing higher proportions of sorbitan monostearate formed organogels in less time and possessed higher consistency and viscosity. All the organogels showed pH in the range of 6.5–7.0 (Table S2).

Stability Studies

The organogels did not show any signs of destabilization at the end of the accelerated and intermediate stability studies. The study was aimed at predicting the long-term stability of the organogels. A stable product should retain its structural integrity when subjected to harsh temperature treatments. The appearance, pH, color, odor, consistency, and texture of the organogels remained unaltered. Hence, the developed organogels can be considered as stable gels. The high stability of the organogels may be attributed to the close packing of sorbitan monostearate molecules which resulted in the formation of the stable 3-D network. Usually, stable network results in the formation of a stable organogel.

Gelation Kinetics Study

Sesame oil showed an absorbance maximum at 451 nm. Hence, the time scan of the organogels was performed at 451 nm for 2.5 min. The organogels were transparent liquid at molten condition (70°C). The molten gels were cooled to room temperature and the absorbance was measured at a regular time interval of 5 s. The absorbance of the samples increased during the sol-to-gel transformation. A near-sigmoidal-shaped curve was obtained when the absorbance values were plotted against time (Fig. 1). Initially, the organogels showed an almost constant absorbance profile, suggesting a lag phase of gel formation. The absorbance values were higher in the organogel containing higher concentrations of sorbitan monostearate. The initial absorbance values of the organogels were in the order of OG1<OG2<OG3<OG4. The time required in reaching the equilibrium phase was considered as the gel setting time. The total time required to achieve the equilibrium phase was in the order of OG1>OG2>OG3>OG4. The time required for gelation per gram of the gel was calculated (Table S3). In general, the gel setting time decreased with the increase in the gelator concentration. The sigmoid curve and long-term equilibrium phase indicated one-dimensional (1-D) crystal growth and followed first-order kinetics (38).

Table II. Composition of the Organogels

Formulations	SMS (% *w/w*)	Sesame oil (% *w/w*)	Metronidazole (% *w/w*)
OG1	15.0	85.0	–
OG2	18.0	82.0	–
OG3	20.0	80.0	–
OG4	22.0	78.0	–
OG1M	15.0	84.0	1.0
OG2M	18.0	81.0	1.0
OG3M	20.0	79.0	1.0
OG4M	22.0	77.0	1.0

Microscopic Studies

The phase contrast micrographs of the organogels are shown in Fig. 2. The organogels showed the presence of needle-shaped structures distributed uniformly throughout the matrix. The sizes of the crystals increased with the increase in the concentration of sorbitan monostearate.

Molecular Properties

The FTIR spectra of the blank organogels and metronidazole-loaded organogels are shown in Figure S2. All the major peaks of the raw materials (sorbitan monostearate and sesame oil) were present in the blank as well as in the drug-loaded organogels and were exactly in match with the reported literature (39, 40). This confirmed that there were no significant interactions between the components at the molecular level. The absorption bands at ~2920 and 2852 cm^{-1} were due to the C–H asymmetric and symmetric stretching vibrations of the sorbitan monostearate and sesame oil. The absorption band at ~1746 cm^{-1} was attributed to the presence of a C=O stretching vibration due to the ester group of the triglycerides present in the sesame oil (40). The absorption band at ~1478 cm^{-1} was due to CH_2 bending vibrations (41). An absorption peak at ~1165 cm^{-1} represented in-plane bending of the aromatic C–H bonds (42). The absorption band at ~717 cm^{-1} was due to the out-of-plane rocking vibrations due to -$(CH_2)_n$- groups (39). The absorption peaks of metronidazole were absent due to its presence in very minute quantity in the drug-loaded organogels (26).

Mechanical Properties

The small-scale deformation study of the developed organogels was performed by viscosity analysis. The organogels showed a shear thinning behavior, confirmed by the decrease in the apparent viscosities at higher shear rates (Fig. 3a). Initially, the apparent viscosity reduced sharply at lower shear rates, but became steady at higher shear rates. This can be explained by the faster reduction in the size of the gelator molecule crystal aggregates as the shear rate was increased. The bigger crystals may break into smaller crystals (fragmentation) and may rearrange themselves into a parallel direction with shear. The breaking of the larger crystals into smaller crystals was confirmed by analyzing the microstructure of the organogels after the viscometric analysis. The micrographs showed the presence of a 3-D network structure of the gelator molecules, but the size of the crystals were much smaller as compared to the crystals observed before the viscometric analysis (Figure S3). During the shear, the crystals align themselves in the direction of the shear which results in the decrease in the viscosity at higher shear rates. This phenomenon has been well explained by Czerwinski, where they

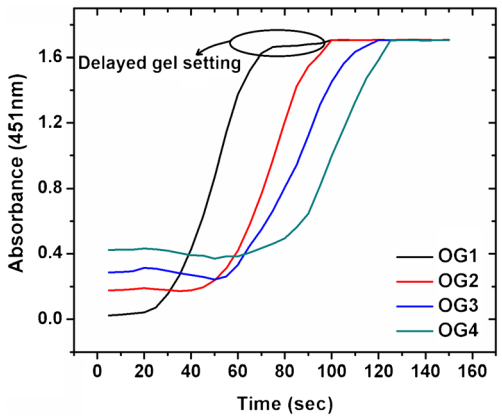

Fig. 1. Gelation kinetics of organogels

have reported breaking of the crystal structure under shear. The crystals reorganize after the removal of the shear and form the network structure (43). Hence, a flow is observed due to the particle–particle interaction resulting in the decrease of the viscosity. The viscosity data was fitted using Ostwald-de Wale power law equation (44)

$$\tau = K \times \gamma^n \tag{1}$$

where, τ is the shear stress (Pa) at γ shear rate (s^{-1}), K is the flow consistency index (Pa s^{-1}), and n is the flow behavior index.

The n value indicated a non-Newtonian flow behavior of the organogels. n value was <1 in all the organogels, which confirmed their pseudoplastic viscous nature (44). The yield stress of the organogels was obtained by fitting the Herschel–Bulkley model (Fig. 3b). Though the values do not specifically represent the strength of the formulations and vary based on the shear rate range used, the yield stress values can be used as an indicative of the comparative firmness of the organogels. The yield stress of the organogels was in the order of OG1<OG2<OG3<OG4, suggesting an increase in the firmness with the increase in the concentration of sorbitan monostearate (Table S4).

The large-scale deformation studies (stress relaxation and spreadability) of the organogels were studied using a static mechanical tester. The stress relaxation study was performed to examine the viscoelastic property of the organogels (Fig. 3c). When a force of 5.0 g was detected, the probe moved a distance of 5 mm, which resulted in the increase of the force value, F_0. The probe was subsequently kept at the said distance for 60 s. The force values decreased with a faster rate initially, which reached to a nearly constant value called as residual force, F_r (45). The percent relaxation of the organogels was calculated by the formula (46)

$$\%\ \text{relaxation} = \left(\frac{F_0 - F_r}{F_0}\right) \times 100 \tag{2}$$

The % relaxation of the organogels was in the range of 80%–84%, which suggested viscoelastic liquid nature of the

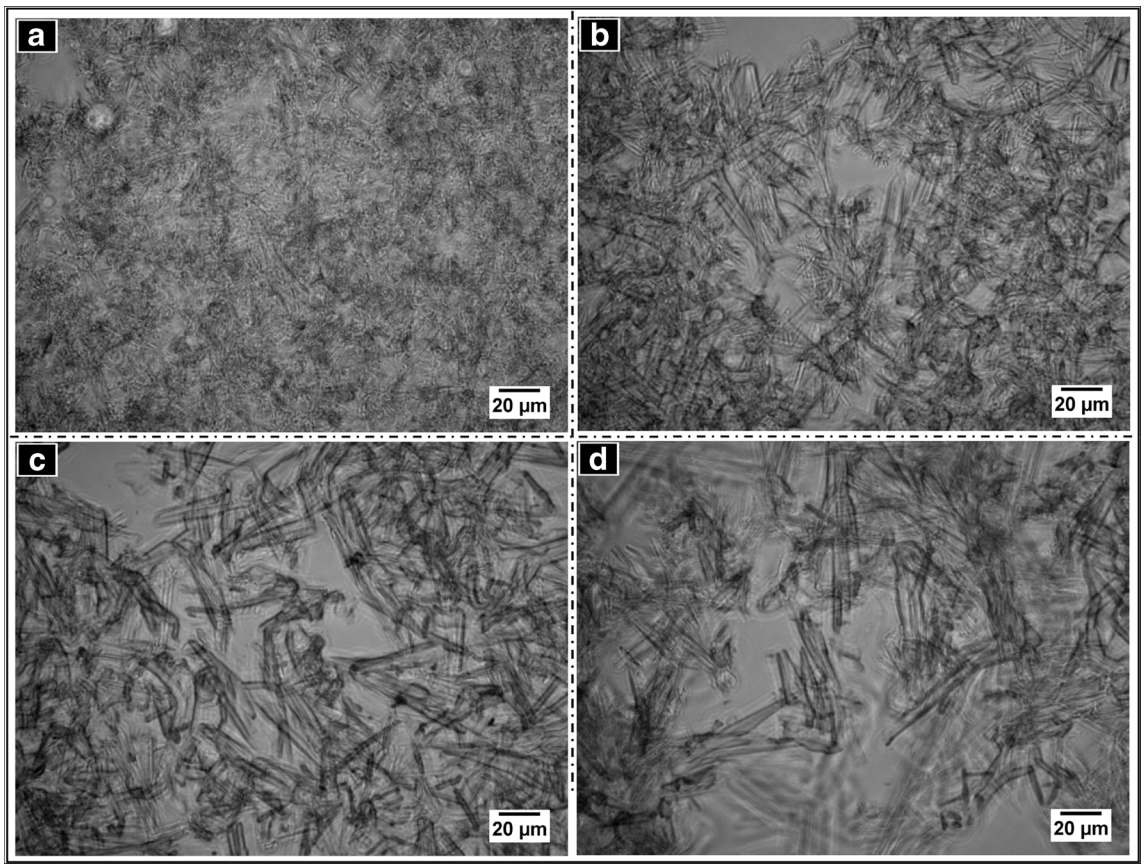

Fig. 2. Phase contrast micrographs of the organogels. **a** OG1, **b** OG2, **c** OG3, and **d** OG4

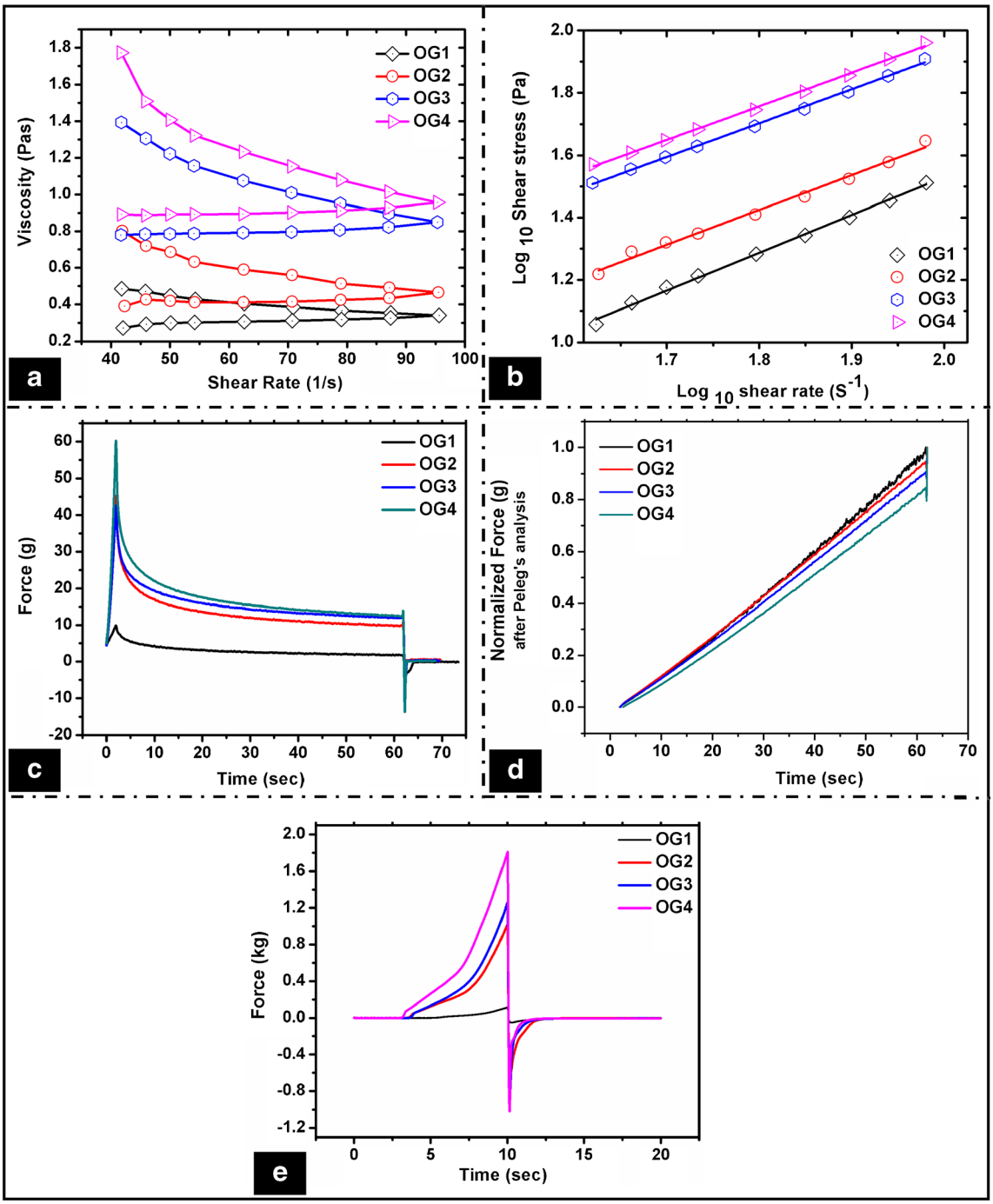

Fig. 3. Mechanical properties of the organogels. Viscosity studies: **a** shear rate-dependent viscosity profile and **b** shear rate-dependent shear stress profile (log–log scale); stress relaxation studies: **c** force–time graph showing stress relaxation of the organogels and **d** normalized force after Peleg's analysis; **e** spreadability studies

organogels (47). Though the differences in the % relaxation was not significant, it was found to be in the sequence of OG1>OG2>OG3>OG4 (Table III). The % relaxation decreased with the increase in the sorbitan monostearate concentration. This can be explained by the increase in the rigidity of the organogels as the concentration of sorbitan monostearate was increased. This resulted in the increase of the stability of the formulations. This was also observed in the viscosity studies.

The stress relaxation data was further analyzed by fitting the force–time data using the modified Peleg's equation (48)

$$\frac{(F_0 - F(t))t}{F_0} = k_1 + k_2 t \tag{3}$$

where k_1 and k_2 indicate the initial rate and the extent of the relaxation, respectively.

Table III. Parameters Obtained from the Stress Relaxation and Spreadability Studies

	Stress relaxation studies							Spreadability studies		
Formulations	F_0 (g)	F_r (g)	% relaxation	k_1	k_2	S	Spreadability (g s^{-1}) ($\times 10^{-3}$)	Firmness (g)	Cohesiveness (g s^{-1})	Stickiness (g)
OG1	9.88	1.64	83.38	2.99	0.85	0.484	5.659	116.637	201.14	−51.485
OG2	42.23	7.99	81.06	1.95	0.74	0.483	1.267	1022.137	2186.766	−603.755
OG3	41.56	7.98	80.80	2.2	0.74	0.483	1.081	1260.056	2674.951	−781.431
OG4	39.25	7.54	80.78	3.05	0.72	0.479	1.003	1809.142	4468.105	−1017.891

The organogels showed a good fit to the Peleg's equation (Fig. 3d). The k_1 value indicates the rate of force decay, whereas the k_2 value gives the complete picture of the stress relaxation behavior of the system. The k_1 value of OG1 was 2.99. As the concentration of the sorbitan monostearate was increased in OG2, there was a sharp decrease in the k_1 value (1.95). Thereafter, an increase in the concentration of sorbitan monostearate resulted in the increase in the k_1 value. There was a decrease in the k_2 value (marker of the overall relaxation) as the concentration was increased. This indicated a decrease in the extent of relaxation when the concentration of sorbitan monostearate was increased, thereby suggesting an increase in the elastic behavior (Table III).

The viscoelastic properties were further quantified by calculating the area under the normalized stress relaxation curve (S). The viscoelastic materials possess an S value in between 0 and 1, where "1" represents a perfect elastic nature and "0" represents a liquid nature. The value of S for the organogels was ~0.48 (Table III). This suggested that the organogels were viscoelastic fluid in nature.

The spreadability profiles of the formulations are shown in Fig. 3e. The inverse of the area under the positive peak curve gives indication about the spreadability of the formulation. The organogels containing a higher sorbitan monostearate concentration showed a lower spreadability and vice versa. This may be attributed to the higher elastic component of the organogels at a higher concentration of the gelator (Table III). The spreadability of the organogels was in the order of OG1>OG2>OG3>OG4.

Various other mechanical properties like firmness (positive peak value), cohesiveness (area under the positive peak), and stickiness (negative peak value) of the organogels were calculated from the spreadability studies. The firmness, cohesiveness, and stickiness of the organogels increased linearly with the increase in the gelator concentration. It was in the order of OG4>OG3>OG2>OG1 (Table III). The results were in accordance to the viscosity and SR studies, which suggested an increase in the elastic component with the increase in the gelator proportion.

The viscoelastic properties of the organogels were further investigated by cyclic creep and recovery studies. The creep phase consisted of the application of a constant shear stress on the samples. The deformation/strain subjected on the sample was recorded as a function of time. During the recovery phase, the applied stress was removed so that the sample recovers from the deformation. The changes in the viscosity (η), creep compliance (J_o), and creep–recovery were calculated from the % strain *vs.* time plots. The above parameters were calculated for 10 repetitive cycles and were plotted against the number of cycles (Fig. 4a). The viscosity (η) of a material corresponds to an increase in the deformation when stress is applied. When the concentration of sorbitan monostearate was highest, there was a steep increase in the viscosity during the second cycle (Fig. 4b–e). Thereafter, there was a continuous decrease in the viscosity. This may be explained by the brittle nature of the gel as compared to the other organogels. The viscosity of the samples was in the order of OG1<OG2<OG3<OG4 (Figure S4a). In general, an increase in the organogelator (sorbitan monostearate) concentration resulted in the increase in the overall viscosity of the organogels.

The creep compliance (J_0) is defined by the ratio of strain to the applied shear stress. It is the deflection observed at the beginning of the deformation and it indicates the pure elasticity at zero time. In general, J_0 represents the elastic viscous components of the soft materials. The organogels showed an increase in the J_0 values upon repetitive creep studies (Fig. 4b–e). The increase in J_0 suggested that the elastic components of the organogels increased with the corresponding loss of the viscous components. The rate of change of J_0 was higher during the initial cycles of the study and then it was lower in the later cycles. Also, it increased with the increase in the gelator concentration from OG1 to OG4. It was in the order of OG1<OG2<OG3<OG4 (Figure S4b). The results were in support of the viscosity results. The change of J_0 component was higher in OG1 and decreased with the increase in the gelator concentration. This suggested that OG1 lost its viscous nature quickly, which may be associated with the deformation in the gel structure when stress was applied. The increase in the gelator concentration increased the rigidity of the organogels, which resulted in the decreased J_0 values. The presence of gelator resisted the flow when stress was applied. The creep compliance has an inverse relation to the stiffness of the formulations. The % decrease in the creep compliance decreased with a corresponding increase in the gelator content. OG1 showed the highest decrease in % creep compliance, which can be associated with its lowest gelator content. This suggested that the stiffness of the organogels increased with the increase in gelator concentration.

The recovery phase deals with the recovery of the formulations from the developed strain during the creep phase in every cycle. The % recovery was calculated using the formula

$$\gamma_{rec} = \frac{(\gamma_c - \gamma_r)}{(\gamma_c - \gamma_0)} \times 100 \quad (4)$$

where γ_r is the strain value at the end of the recovery phase of each cycle, γ_0 is the strain value at the start of each creep cycle, and γ_c is the strain value at the end of each creep cycle.

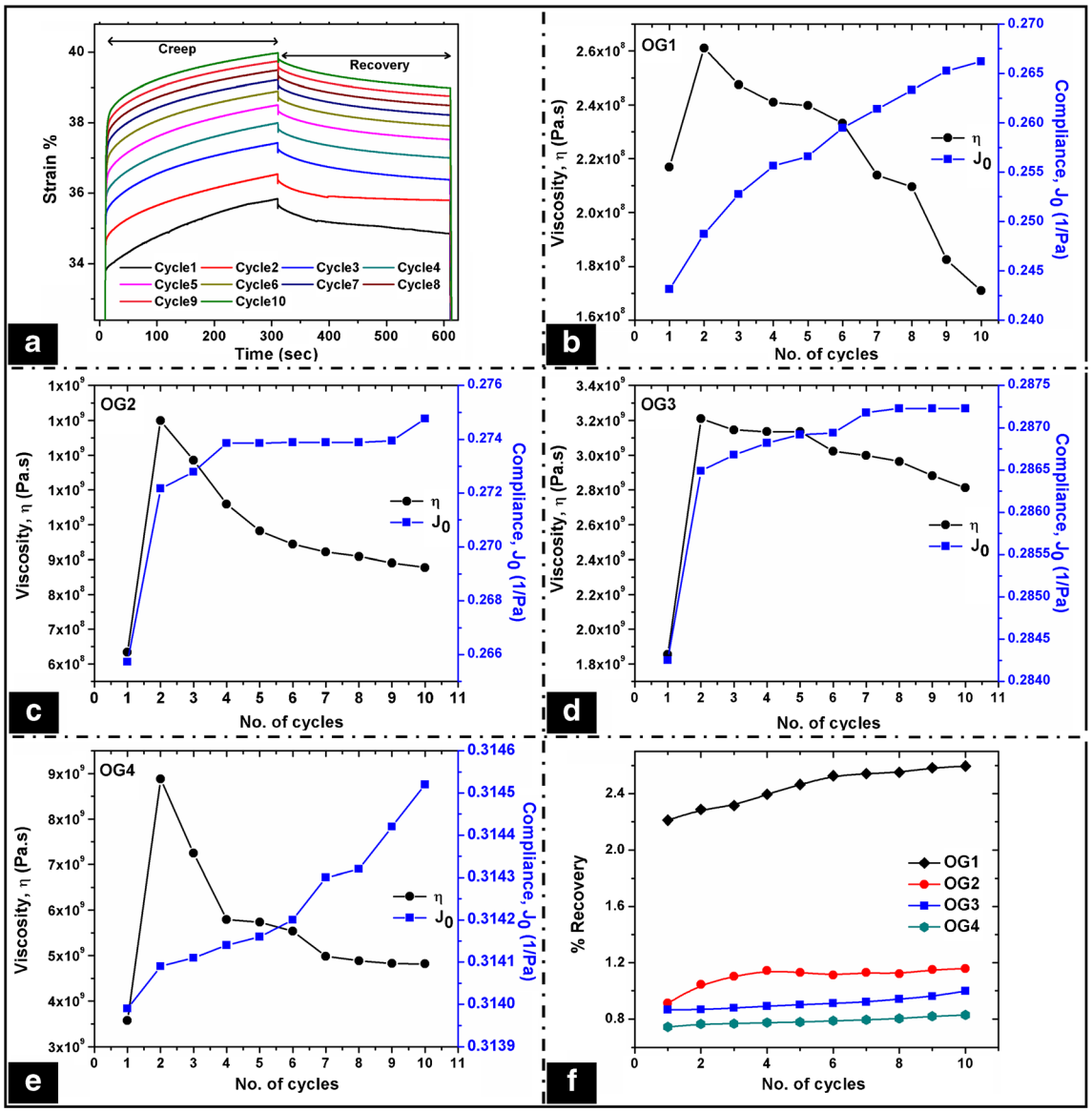

Fig. 4. Creep and recovery studies of the organogels. **a** Creep–recovery profile of a representative organogel; viscosity and compliance profile obtained from the creep study of **b** OG1, **c** OG2, **d** OG3, and **e** OG4. **f** recovery profile of the organogels

In general, recovery study represents the recovery of the viscoelastic component of the formulations after the application of the shear. The organogels showed very low recovery (0.8%–2.2%) which may be due to the higher solid-like nature of the formulations. The creep–recovery was higher in the organogels containing lower concentrations of sorbitan monostearate. The recovery was in the order of OG1>OG2>OG3>OG4 (Fig. 4f). In the early stages of the study, a detectable % recovery was observed, but leads to almost constant values with the increase in the number of cycles.

Thermal Properties

The melting points of the organogels increased with the increase in the gelator concentration in the organogels. The organogels showed their melting point in the range of 49°C–54°C. The higher melting points of the organogels with higher gelator fractions indicated higher thermal stability of the organogels. The melting point of the organogels was in the order of OG4>OG3>OG2>OG1 (Table S5).

The thermal events of sorbitan monostearate, sesame oil, and the organogels were evaluated using a differential scanning calorimeter (Fig. 5). The melting events [$T_{onset,m}$ (onset temperature), T_m (melting temperature), ΔH_m (melting enthalpy), ΔS_m (melting entropy)] and crystallization events [$T_{onset,c}$ (onset temperature), T_c (crystallization temperature), ΔH_c (crystallization enthalpy), ΔS_c (crystallization entropy)] of the organogels were calculated using the NETZSCH Proteus software (Table IV). The thermal profile of sorbitan monostearate shows an endothermic and an exothermic peak at 51°C and 45°C, respectively, during the heating and cooling cycles (8, 49). Sorbitan monostearate showed endothermic and exothermic peaks at 57.2°C and 50.1°C during the heating and cooling cycles, respectively. Sesame oil showed three less intense endothermic peaks at ~41°C, 101°C, and 148°C

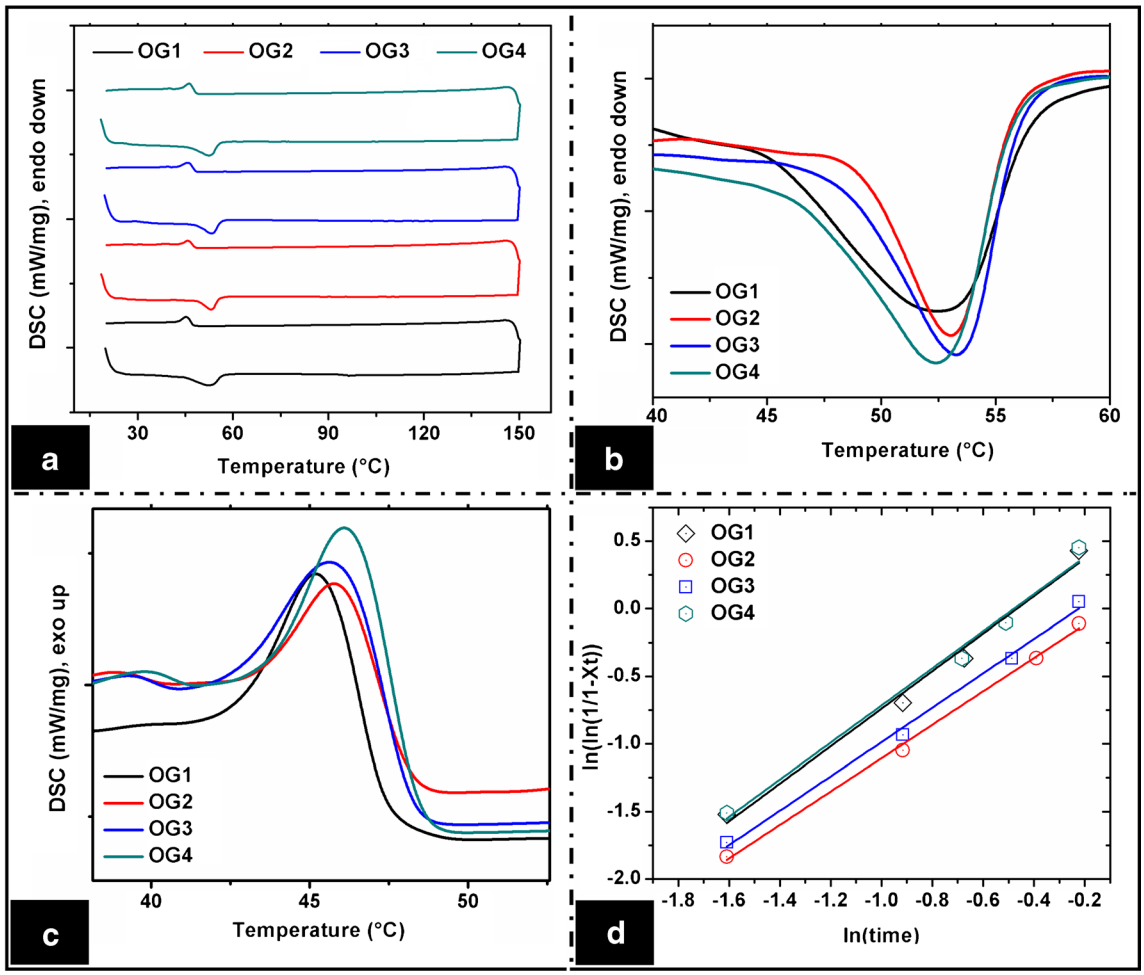

Fig. 5. DSC thermograms. **a** Complete thermogram, **b** thermogram showing the melting temperatures of sorbitan monostearate, **c** thermogram showing the crystallization temperature of sorbitan monostearate, and **d** Avrami equation fitting curves

(Figure S5). The heating DSC curves of the organogels showed a sharp endothermic peak in the temperature range of 52°C–54°C, whereas the cooling DSC curves showed a sharp exothermic peak in the temperature range of 45°C–47°C (Fig. 5b, c). The endothermic and the exothermic peaks can be assigned to the melting and the crystallization temperatures of sorbitan monostearate, respectively. This confirmed the presence of sorbitan monostearate molecules in their near-native state in the organogel matrices. The corresponding peaks obtained in the organogels shifted slightly towards the lower temperature, which may be associated with the structural changes during the organogel preparation in sorbitan monostearate at the molecular level. The peaks observed in sesame oil were not visible in the organogels, which may be ascribed to the presence of the highly crystalline sorbitan monostearate. Due to the thermal hysteresis, the melting and crystallization peak positions varied. The melting and the crystallization enthalpies and entropies were measured using the area under the respective peaks (Table IV). The enthalpy (ΔH_m) and the entropy (ΔS_m) of the organogels

Table IV. DSC Studies of the Organogels

	Melting, endotherm				Crystallization, exotherm				Crystallization kinetics (Avrami equation)	
Formulations	$T_{onset,m}$ (°C)	T_m (°C)	ΔH_m (J g^{-1})	ΔS_m (J g^{-1} K^{-1})	$T_{onset,c}$ (°C)	T_c (°C)	ΔH_c (J g^{-1})	ΔS_c (J g^{-1} K^{-1})	n	R^2
OG1	45	52.5	5.193	0.098	42.9	45.3	0.887	0.0195	1.386	0.981
OG2	48.8	53.1	5.301	0.099	43.9	45.9	0.901	0.0196	1.234	0.996
OG3	48.7	53.4	5.410	0.101	43.3	45.8	1.036	0.0226	1.269	0.994
OG4	46.5	52.5	5.448	0.103	44.3	46.2	1.180	0.0255	1.371	0.979

increased with the increase in the concentration of sorbitan monostearate. It was in the order of OG4>OG3>OG2>OG1. Hence, it can be said that the thermodynamic stability of the organogels increased as the gelator concentration was increased.

The Avrami equation was used to study the crystallization kinetics of the organogels (50)

$$\ln\left(\ln\left({}^{1}/_{1-X_t}\right)\right) = \ln K + n\ln t \tag{5}$$

where X_t is the volume fraction of the gelator at time t and K is the crystallization rate constant. In general, K is influenced by both nucleation and crystal growth (s^{-1}); n is the Avrami exponent.

The n value represents the nucleation and the dimension of the crystal growth. It ranges from 1 to 3 depending on the shape and growth of the crystals. An integer value of n=1, 2, and 3 represents the formation of rod-shaped crystals (1-D), disk-shaped crystals (two-dimensional (2-D)), and spherical crystals (3-D), respectively. A non-integer value indicated the formation of irregular-shaped crystals. The degree of gelator transformation (X_t) was calculated from the crystallization exothermic peaks of the DSC thermograms using the following equation:

$$X_t = \frac{H_t}{H_E} = \frac{\int_{t_i}^{t} \Delta H_c dt}{\int_{t_i}^{t_f} \Delta H_c dt} \tag{6}$$

where H_t is the heat associated with the crystallization up to time t and H_E is the total heat involved during the crystallization process.

The slope value of the Avrami plots gives the Avrami exponents (n value) (Fig. 5d, Table IV). The organogels showed non-integer exponent values and were in between 1.2 and 1.4. This suggested predominant first-order nucleation kinetics and formation of 1-D crystal formation (51). The first-order nucleation kinetics indicated that the nucleation of the crystals did not occur instantaneously, but was a continuous process during gelation. Hence, the nucleation can either be

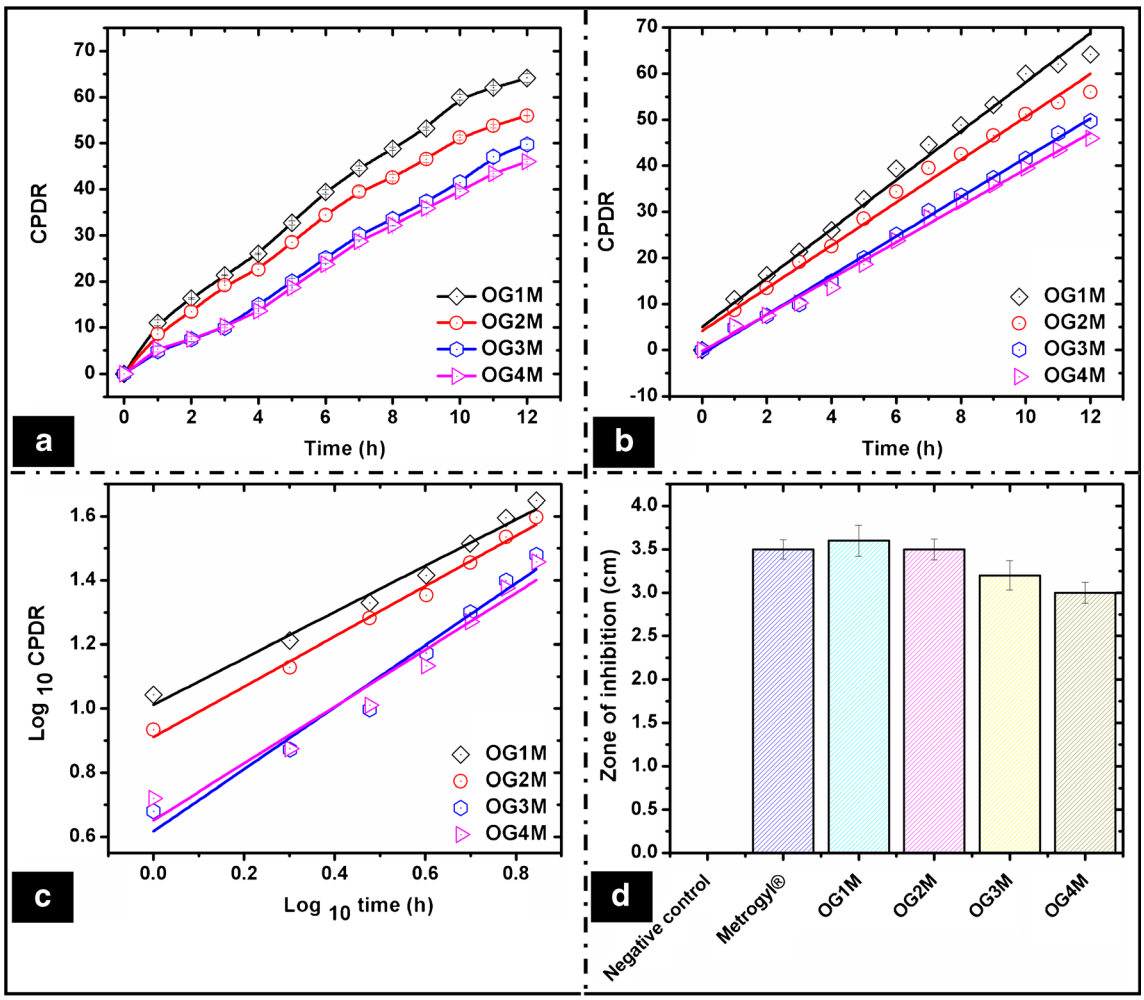

Fig. 6. *In vitro* drug release studies. **a** CPDR, **b** zero-order release kinetics, **c** Korsmeyer–Peppas model fitting, and **d** antimicrobial assay

heterogeneous or simultaneous nucleation (52). Phase contrast micrographs (Fig. 1) also showed the evidence of heterogeneous nucleation during gelation. The change in the n value suggested a change in the order of the crystal growth. The non-integer Avrami exponent values indicated the existence of irregular-shaped crystals. It also suggested the existence of secondary crystallization by the heterogeneous nucleation process during the formation of the organogels. The R^2 values decreased with the increase in the concentration of sorbitan monostearate. This suggested the existence of secondary crystallization process during gelation (Table IV) (52). Hence, it can be stated that the change in the concentration of the gelator regulated the secondary crystallization.

The mechanism of gelation of sorbitan monostearate in sesame oil was predicted by gelation kinetics studies (Fig. 1). The heterogeneous nucleation observed during the gelation process was associated with 1-D crystal growth. Sorbitan monostearate molecules arranged themselves as toroidal inverse vesicles, which on further cooling led to the development of rod-shaped tubules (8, 53). It reduced the interfacial tension during the crystal growth. The non-covalent cross-linking and mechanical entanglement between the gelator molecule and the oil phase led to form an ordered arrangement at the gelator–oil interface. This resulted in formation of the 3-D gelator network (54).

Biocompatibility Study

The leachant of the organogels was prepared in phosphate buffer (pH 7.2) and was tested for the cell viability against HaCaT cells. The MTT assay confirmed that the cells were viable when put in contact with the organogel extracts (Figure S6). The variation in the cell viability index in comparison to the control was statistically insignificant ($p>0.05$). Also, there were no significant changes in the morphology of the cells in the presence of the extracts of the organogels as compared to the control. The above results suggested the biocompatible nature of the formulations.

In vitro Drug Release

The cumulative percent drug release (CPDR) of the drug from the organogel was in the order of OG1M>OG2M>OG3M>OG4M (Fig. 6a). The release study indicated that the rate of drug release was higher in the organogels containing lower gelator concentration. The percentage release of the drug decreased from 64% to 46% when the concentration of sorbitan monostearate was increased from 15% to 22% *w*/*w* (Table S6). The gelator network might have hindered the migration (diffusion) of the drug, resulting in its lower release with the increase in the gelator concentration. The release studies suggested that the release of the drugs can be controlled by tailoring the concentration of sorbitan monostearate in the organogels. Hence, the developed organogels can be considered as potential matrices for controlled release applications. Shah *et al.* reported a controlled release of metronidazole in 12 h which was much less (<40% *w*/*w*) (13) as compared to the formulations (45%–65% *w*/*w*) reported in this study. The release behavior of the drug from the organogel matrix was evaluated using various release kinetic models. The release of the drug followed zero-order release kinetics in all the organogels ($R^2>0.95$) (Fig. 6b). This confirmed concentration-independent diffusion-mediated release of metronidazole from the organogel matrices (55). The zero-order release kinetics from the organogels was expected due to the poor solubility of metronidazole in sesame oil (56, 57).

The Korsmeyer–Peppas (KP) model was used to investigate the mechanism of drug diffusion (Fig. 6c). The type of drug diffusion from the organogels was estimated by fitting the 60% of the total drug released data in the Korsmeyer–Peppas model (58). The diffusion coefficient (n value) of the organogels varied from 0.61 to 0.78, which suggested a non-Fickian release behavior (Table S6). Hence, the release of metronidazole can be attributed mainly to the diffusion or permeation of the drug through the organogel matrix.

Antimicrobial Test

The antimicrobial assay of the metronidazole-loaded organogels was performed against *E. coli.* The zone of inhibition obtained after incubating the petri plates was comparable to Metrogyl®. The negative controls did not show any zone of inhibition (Fig. 6d). The results suggest that the organogels may be tried as matrices for drug delivery.

CONCLUSION

Sorbitan monostearate–sesame oil-based organogels were prepared and characterized thoroughly by investigating various molecular, mechanical, and thermal properties. The micrographs of the organogels showed the presence of needle-shaped crystal structures of sorbitan monostearate. The organogels were stable, smooth, and biocompatible. They were amorphous in nature and showed a non-Newtonian shear thinning flow behavior. The stability (long-term and thermal) and the mechanical properties (viscosity and firmness) increased with the increase in the organogelator (sorbitan monostearate) concentration. The metronidazole-loaded organogels showed diffusion-mediated release of drug from the organogel matrix. The antimicrobial assay showed a good inhibitory action of the drug-loaded organogels against *E. coli.* The critical gelator concentration of sorbitan monostearate was 15% *w*/*w*, which was much lower as compared to the reported literatures. The developed organogels showed a controlled release of metronidazole (46%–64% *w*/*w*) compared to the previously reported sorbitan monostearate-based organogels. Hence, the developed organogels can be considered as probable matrices for a controlled release of the antimicrobials for topical application.

ACKNOWLEDGMENTS

The authors gratefully acknowledge the financial assistance received from the project SR/FT/LS-171/2009, sanctioned by the Science and Engineering Research Board (SERB), Govt. of India.

REFERENCES

1. Pal A, Dey J. Water-induced physical gelation of organic solvents by N-(n-alkylcarbamoyl)-l-alanine amphiphiles. Langmuir. 2011;27(7):3401–8.
2. Landry CJT, Coltrain BK, Brady BK. In situ polymerization of tetraethoxysilane in poly (methyl methacrylate): morphology and dynamic mechanical properties. Polymer. 1992;33(7):1486–95.
3. Placin F, Colomès M, Desvergne JP. A new example of small molecular non-hydrogen bonding gelators for organic solvents. Tetrahedron Lett. 1997;38(15):2665–8.
4. George M, Weiss RG. Low molecular-mass organic gelators. Mol Gels. 2006:449–551.
5. Hughes NE, Marangoni AG, Wright AJ, Rogers MA, Rush JWE. Potential food applications of edible oil organogels. Trends Food Sci Technol. 2009;20(10):470–80.
6. Stanos SP. Topical agents for the management of musculoskeletal pain. J Pain Symptom Manag. 2007;33(3):342–55.
7. Patil VV. Span-60 based organogels as probable matrices for transdermal/topical delivery systems 2011.
8. Murdan S, Gregoriadis G, Florence AT. Novel sorbitan monostearate organogels. J Pharm Sci. 1999;88(6):608–14.
9. Daniel J, Rajasekharan R. Organogelation of plant oils and hydrocarbons by long-chain saturated FA, fatty alcohols, wax esters, and dicarboxylic acids. J Am Oil Chem Soc. 2003;80(5):417–21.
10. Toro-Vazquez J, Morales-Rueda J, Dibildox-Alvarado E, Charo-Alonso M, Alonzo-Macias M, Gonzalez-Chavez M. Thermal and textural properties of organogels developed by candelilla wax in safflower oil. J Am Oil Chem Soc. 2007;84(11):989–1000.
11. Bhattacharya C, Kumar N, Sagiri SS, Pal K, Ray SS. Development of span 80–tween 80 based fluid-filled organogels as a matrix for drug delivery. J Pharm bioallied Sci. 2012;4(2):155.
12. Wright AJ, Marangoni AG, Garti N. Vegetable oil-based ricinelaidic acid organogels—phase behavior, microstructure and rheology. In: Edible oleogels: structure and health implications. Urbana: AOCS Press; 2011. p. 81–99.
13. Shah DK, Sagiri SS, Behera B, Pal K, Pramanik K. Development of olive oil based organogels using sorbitan monopalmitate and sorbitan monostearate: a comparative study. J Appl Polym Sci. 2013;129(2):793–805.
14. Peyronel F, Marangoni AG. In search of confectionary fat blends stable to heat: hydrogenated palm kernel oil stearin with sorbitan monostearate. Food Res Int. 2014;55:93–102.
15. Bedigian D, Seigler DS, Harlan JR. Sesamin, sesamolin and the origin of sesame. Biochem Syst Ecol. 1985;13(2):133–9.
16. Wei W, Qi X, Wang L, Zhang Y, Hua W, Li D, *et al*. Characterization of the sesame (Sesamum indicum L.) global transcriptome using Illumina paired-end sequencing and development of EST-SSR markers. BMC Genomics. 2011;12(1):451.
17. Periasamy S, Chien S-P, Chang P-C, Hsu D-Z, Liu M-Y. Sesame oil mitigates nutritional steatohepatitis via attenuation of oxidative stress and inflammation: a tale of two-hit hypothesis. J Nutr Biochem. 2014;25(2):232–40.
18. Suja K, Jayalekshmy A, Arumughan C. Antioxidant activity of sesame cake extract. Food Chem. 2005;91(2):213–9.
19. Cheung SCM, Szeto YT, Benzie IF. Antioxidant protection of edible oils. Plant Foods Hum Nutr. 2007;62(1):39–42.
20. Chung CH, Yee YJ, Kim DH, Kim HK, Chung DS. Changes of lipid, protein, RNA and fatty acid composition in developing sesame (Sesamum indicum L.) seeds. Plant Sci. 1995;109(2):237–43.
21. Tsuruoka N, Kidokoro A, Matsumoto I, Abe K, Kiso Y. Modulating effect of sesamin, a functional lignan in sesame seeds, on the transcription levels of lipid-and alcohol-metabolizing enzymes in rat liver: a DNA microarray study. Biosci Biotechnol Biochem. 2005;69(1):179–88.
22. Chen PR, Chien KL, Su TC, Chang CJ, Liu T-L, Cheng H, *et al*. Dietary sesame reduces serum cholesterol and enhances antioxidant capacity in hypercholesterolemia. Nutr Res. 2005;25(6):559–67.
23. Periasamy S, Yang S-S, Chen S-Y, Chang C-C, Liu M-Y. Prophylactic sesame Oil attenuates sinusoidal obstruction syndrome by inhibiting matrix metalloproteinase-9 and oxidative stress. J Parenter Enter Nutr. 2013;37(4):529–37.
24. Saleem MT, Chetty MC, Kavimani S. Antioxidants and tumor necrosis factor alpha-inhibiting activity of sesame oil against doxorubicin-induced cardiotoxicity. Therapeutic advances in cardiovascular disease. 2014;1753944713516532.
25. Haering G, Luisi PL. Hydrocarbon gels from water-in-oil microemulsions. J Phys Chem. 1986;90(22):5892–5.
26. Singh VK, Pal K, Pradhan DK, Pramanik K. Castor oil and sorbitan monopalmitate based organogel as a probable matrix for controlled drug delivery. J Appl Polym Sci. 2013;130(3):1503–15.
27. Singh VK, Ramesh S, Pal K, Anis A, Pradhan DK, Pramanik K. Olive oil based novel thermo-reversible emulsion hydrogels for controlled delivery applications. J Mater Sci Mater Med. 2013;1–19.
28. Singh VK, Anis A, Al-Zahrani S, Pradhan DK, Pal K. FTIR, electrochemical impedance and iontophoretic delivery analysis of guar gum and sesame oil based bigels. Int J Electrochem Sci. 2014;9:5640–50.
29. Singh VK, Anis A, Al-Zahrani S, Pradhan DK, Pal K. Molecular and electrochemical impedance spectroscopic characterization of the carbopol based bigel and its application in iontophoretic delivery of antimicrobials. Int J Electrochem Sci. 2014;9:5049–60.
30. Neves J, Da Silva MV, Gonçalves MP, Amaral MH, Bahia MF. Rheological properties of vaginal hydrophilic polymer gels. Curr Drug Deliv. 2009;6(1):83–92.
31. Carr L, Tadini C. Influence of yeast and vegetable shortening on physical and textural parameters of frozen part baked French bread. LWT Food Sci Technol. 2003;36(6):609–14.
32. van der Laan S, Feringa BL, Kellogg RM, van Esch J. Remarkable polymorphism in gels of new azobenzene bis-urea gelators. Langmuir. 2002;18(19):7136–40.
33. Pal K, Banthia AK, Majumdar DK. Preparation and characterization of polyvinyl alcohol-gelatin hydrogel membranes for biomedical applications. AAPS PharmSciTech. 2007;8(1):E142–6.
34. Nayak PG, Paul P, Bansal P, Kutty NG, Pai KSR. Sesamol prevents doxorubicin-induced oxidative damage and toxicity on H9c2 cardiomyoblasts. J Pharm Pharmacol. 2013;65:1083–93.
35. Singh VK, Anis A, Banerjee I, Pramanik K, Bhattacharya MK, Pal K. Preparation and characterization of novel carbopol based bigels for topical delivery of metronidazole for the treatment of bacterial vaginosis. Mater Sci Eng C. 2014.
36. Singh VK, Sagiri SS, Pal K, Khade SM, Pradhan DK, Bhattacharya MK. Gelatin-carbohydrate phase-separated hydrogels as bioactive carriers in vaginal delivery: preparation and physical characterizations. J Appl Polym Sci. 2014.
37. Behera B, Patil V, Sagiri S, Pal K, Ray S. Span-60-based organogels as probable matrices for transdermal/topical delivery systems. J Appl Polym Sci. 2012;125(2):852–63.
38. Nielsen L, Khurana R, Coats A, Frokjaer S, Brange J, Vyas S, *et al*. Effect of environmental factors on the kinetics of insulin fibril formation: elucidation of the molecular mechanism. Biochemistry. 2001;40(20):6036–46.
39. Deng D-H, Xu L, Ye Z-H, Cui H-F, Cai C-B, Yu X-P. FTIR spectroscopy and chemometric class modeling techniques for authentication of Chinese sesame Oil. J Am Oil Chem Soc. 2012;89(6):1003–9.
40. Savrık SA, Balköse D, Ülkü S. Synthesis of zinc borate by inverse emulsion technique for lubrication. J Therm Anal Calorim. 2011;104(2):605–12.
41. Desai J, Alexander K, Riga A. Characterization of polymeric dispersions of dimenhydrinate in ethyl cellulose for controlled release. Int J Pharm. 2006;308(1):115–23.
42. Sahoo S, Chakraborti C, Naik S, Mishra S, Nanda U. Structural analysis of ciprofloxacin-carbopol polymeric composites by X-Ray diffraction and Fourier transform infra-red spectroscopy. Trop J Pharma Res. 2011;10(3):273.
43. Czerwinski F. The basics of modern semi-solid metal processing. JOM. 2006;58(6):17–20.
44. Halley PJ, Mackay ME. Chemorheology of thermosets—an overview. Polym Eng Sci. 1996;36(5):593–609.
45. Drissi-Alami H, Aroztegui M, Lemagnen G, Larrouture D, Casahoursat L. The effects of the tabletting machine speed on physical characteristics of pharmaceutical powders. J Pharm Belg. 1993;48(1):43.
46. Ebba F, Piccerelle P, Prinderre P, Opota D, Joachim J. Stress relaxation studies of granules as a function of different lubricants. Eur J Pharm Biopharm. 2001;52(2):211–20. doi:10.1016/S0939-6411(01)00171-0.

47. Bellido G, Hatcher D. Asian noodles: revisiting Peleg's analysis for presenting stress relaxation data in soft solid foods. J Food Eng. 2009;92(1):29–36.
48. Peleg M. Characterization of the stress relaxation curves of solid foods. J Food Sci. 1979;44(1):277–81. doi:10.1111/j.1365-2621.1979.tb10062.x.
49. Bunjes H, Koch MH, Westesen K. Effects of surfactants on the crystallization and polymorphism of lipid nanoparticles. Springer: Molecular Organisation on Interfaces; 2002. p. 7–10.
50. Bag BG, Dinda SK, Dey PP, Mallia VA, Weiss RG. Self-assembly of esters of arjunolic acid into fibrous networks and the properties of their organogels. Langmuir. 2009;25(15):8663–71. doi:10.1021/la8042796.
51. Huang X, Terech P, Raghavan SR, Weiss RG. Kinetics of 5α-cholestan-3β-yl N-(2-naphthyl)carbamate/n-alkane organogel formation and its influence on the fibrillar networks. J Am Chem Soc. 2005;127(12):4336–44. doi:10.1021/ja0426544.
52. Lopes-da-Silva JA, Coutinho JAP. Analysis of the isothermal structure development in waxy crude oils under quiescent conditions. Energy Fuel. 2007;21(6):3612–7. doi:10.1021/ef700357v.
53. Rogers MA. Novel structuring strategies for unsaturated fats–meeting the zero-trans, zero-saturated fat challenge: a review. Food Res Int. 2009;42(7):747–53.
54. Ariyaprakai S, Limpachoti T, Pradipasena P. Interfacial and emulsifying properties of sucrose ester in coconut milk emulsions in comparison with Tween. Food Hydrocoll. 2013;30(1):358–67.
55. Varshosaz J, Tabbakhian M, Salmani Z. Designing of a thermosensitive chitosan/poloxamer in situ gel for ocular delivery of ciprofloxacin. Open Drug Deliv J. 2008;2:61–70.
56. Dash S, Murthy PN, Nath L, Chowdhury P. Kinetic modeling on drug release from controlled drug delivery systems. Acta Pol Pharm. 2010;67(3):217–23.
57. Ciolino JB, Hoare TR, Iwata NG, Behlau I, Dohlman CH, Langer R, *et al*. A drug-eluting contact lens. Invest Ophthalmol Vis Sci. 2009;50(7):3346–52.
58. Hesaraki S, Moztarzadeh F, Nezafati N. Evaluation of a bioceramic-based nanocomposite material for controlled delivery of a non-steroidal anti-inflammatory drug. Med Eng Phys. 2009;31(10):1205–13. doi:10.1016/j.medengphy.2009.07.019.